A seismic modelling study for Antarctic subglacial lake exploration

S. Picotti

Istituto Nazionale di Oceanografia e Geofisica Sperimentale – OGS, Trieste, Italy

(Received March 29, 2004; accepted October 1, 2004)

ABSTRACT The recent interest of Antarctic research on subglacial lakes requires a better understanding of their geological context, i.e., their relation to basement structures, the mechanism of the sedimentary processes, and the possible occurrence of free-gas or gas-hydrate bearing layers. The multichannel seismic method is a useful investigation tool for these purposes. This study was undertaken to provide a procedure for designing suitable seismic surveys, aimed at determining the location and the morphology of Antarctic subglacial lakes by employing a reasonable amount of resources. This procedure involves numerical simulation of synthetic seismograms, AVO analysis, ray-tracing and travel-time tomography. In particular, we applied this methodology to the seismic characterisation of Lake Vostok, and the following optimal basic configuration is advisable: two arrays of 6 geophones spaced at 100 m intervals, the first one placed at 500 m from the source and the second one at 3 km from the source. Shifting both source and arrays 1 km away after each shot, we are able to obtain a sufficient ray coverage at the bottom of the lake, and define the ice-water, water-sediment and sediment-bedrock interfaces with an accuracy of about 16 m. This study also provides a general methodology for optimising seismic surveys.

1. Introduction

The OGS (Istituto Nazionale di Oceanografia e Geofisica Sperimentale) leads a research unit within a broader project funded by the PNRA (Programma Nazionale di Ricerche in Antartide) on the Exploration of Antarctic subglacial lakes, coordinated by the University of Milan, whose objective is to design and to execute multichannel seismic surveys aimed at defining the geometry of these lakes. A large number of subglacial lakes were discovered in Antarctica (Fig. 1a) using georadar methods (Siegert *et al.*, 1996; Siegert, 2000), so today the problem is to understand their inner structures and geologic context, and also their potential as sources of information for the reconstruction of the glacial history of Antarctica. These studies focus on the seismic exploration of Lakes Vostok and Concordia (Fig. 1a) for the following reasons:

1. both these lakes are located in a strategic position, very close, respectively, to the stations of Dome C (Italy-France) and Vostok (Russia), where the essential logistic facilities can be provided;
2. Lake Vostok is located beneath nearly 4 km of glacial ice, some hundreds of meters below the base of a well, and is therefore the first candidate for a direct exploration and sampling;
3. up to now, the existence of Lake Concordia is merely speculative. In fact, the only experimental evidence is the flat shape of the glacial cap basement, defined using Radio Echo

Sounding (RES) methods. The final response of the existence of Lake Concordia can be provided only by the seismic survey method.

In order to reconstruct the origin and the evolution of Antarctic subglacial lakes, the analysis of sediments on the bottom is an important source of information. This analysis regards the depositional mechanisms, the sedimentation rates, and the eventual correlation with the alternation of glacial and interglacial phases. The interest extends also to the possible presence of micro-organisms, to studies related to paleo-environmental problems and to the heat flow (analysis of the ice-core) and, finally, to the possible presence of meteoritic material, cosmic powder and free-gas or gas-hydrate bearing layers. The seismic surveys carried out in 1964 (Kapitsa *et al*., 1996) and those realised by the PMGRE (Polar Marine Geological Research Expedition) and RAE (Russian Antarctic Expedition) between 1995 and 2001 (Masolov *et al*., 1999; Fig. 1b), allowed the localisation of a sediment package in some zones of Lake Vostok, interposed between the layer of water and the basement. The techniques employed in these surveys were the Vertical Seismic Profiling (VSP) and Reflection Seismic Sounding (RSS) methods. However, the knowledge of the distribution of the sedimentary sequences and their depositional geometry is rather fragmentary or altogether absent. Therefore, there is a need for suitable models that study the seismic response of Antarctic subglacial lakes and to plan multichannel seismic surveys aimed at recovering their location and morphology.

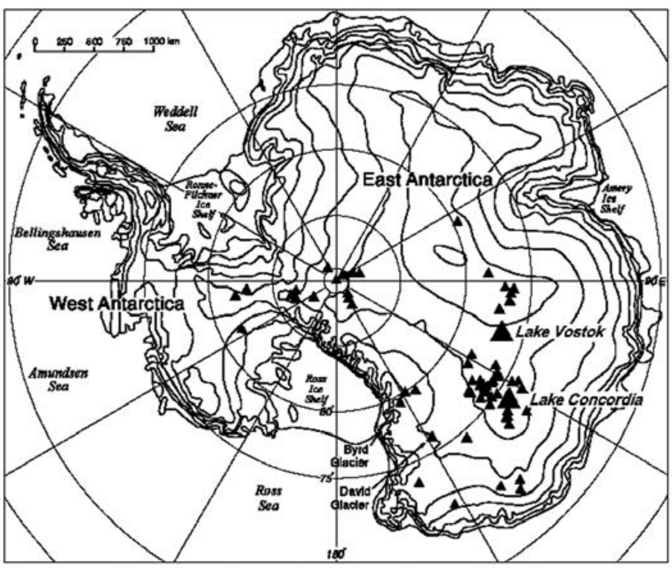

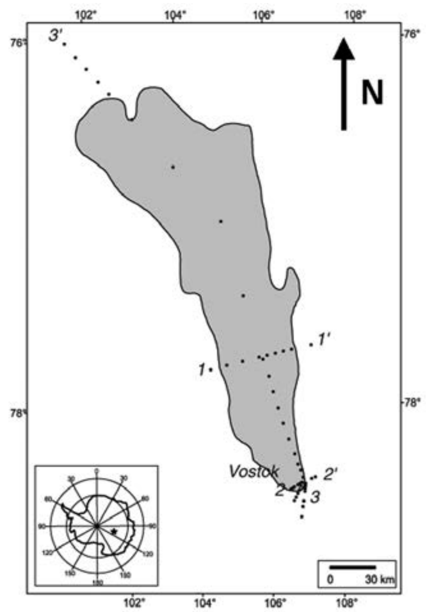

Fig. 1 - a) The distribution of Antarctic subglacial lakes. b) Lake Vostok is located in East Antarctica between 76.2°S/102°E and 78.4°S/108°E, beneath nearly 4 km of glacial ice. The dots indicate the location of the seismic data acquired in the area [see Masolov *et al.* (1999) for more details].

With the purpose of driving a future multichannel seismic survey on Lakes Vostok and Concordia, a modelling study to design a suitable seismic acquisition geometry has been recently undertaken at OGS. The application of the seismic method on the Antarctic plateau implies resolving noticeable operative problems. This is essentially due to the technical and logistic difficulties, induced by the extreme environmental conditions, i.e., low temperatures, problems in transporting the instrumentation, the coupling of sources and receivers with the surface. Therefore, a preliminary analysis is required, in order to avoid a waste of resources. This study, performed using a seismic model of Lake Vostok, a wave modelling commercial package (Tesseral 2-D; Tesseral Technologies Inc.) and a seismic tomographic software (CAT-3D, realised by the staff of the REDS group at OGS), allowed us to optimise the seismic survey, in order to obtain good results with reasonable operational efforts.

The paper is organised as follows. Firstly, we designed the synthetic model of Lake Vostok by using the available seismic information and the seismic properties derived from poroelasticity and viscoelasticity theories (Carcione and Gei, 2003). Next, we carried out a numerical wave simulation of a single shot in the seismic model, to estimate the AVO (Amplitude Versus Offset) response of the Ice-Water (I-W), Water-Sediments (W-S) and Sediments-Basement (S-B) interfaces. On the basis of this information, we optimised the seismic acquisition configuration, to have the best S/N ratio, a sufficient ray coverage at the lake bottom and the appropriate characteristics for a faithful tomographic inversion. Then, we simulated a seismic survey by doing a ray-tracing through the model and we reconstructed the Lake Vostok geometry by performing a tomographic inversion of the I-W, W-S and S-B reflected arrivals. Finally, we estimated the velocity and depth deviations between the inverted model and the initial model. The aim of this analysis is to show that, by using appropriate seismic acquisition parameters, it is possible to define a typical Antarctic subglacial structure, acceptably accurately, even when employing a minimum amount of resources.

2. Travel-time tomography

The adopted tomographic algorithm (CAT-3D), based on the SIRT method and the minimum-time ray tracing, can estimate the velocity field and the reflector structure in sequence (Vesnaver *et al.*, 1999). The model is a blocky one, with voxels (3D case) or pixels (2D case) where the velocity is assumed constant. The base and top of the pixels/voxels define the reflecting/refracting interfaces, that may be curved and dipping interfaces. The tomographic algorithm is based on the iterative procedure shown in Fig. 2. The procedure starts from an initial model, generally with constant velocities within the layers and horizontally flat interfaces, and a set of interpreted events picked on the seismic data. Then, we invert the picked travel-times and update the model, until the variations of velocity and depth of interfaces become sufficiently small. The interface estimation follows the principle of minimum dispersion of the reflected (or refracted) points obtained from the estimated velocities and, within each single step, we can optimise the velocity grid by using an adaptive method for the grid updating (Fig. 2). Reflected, refracted, direct waves and both P and S waves may be analysed by the package.

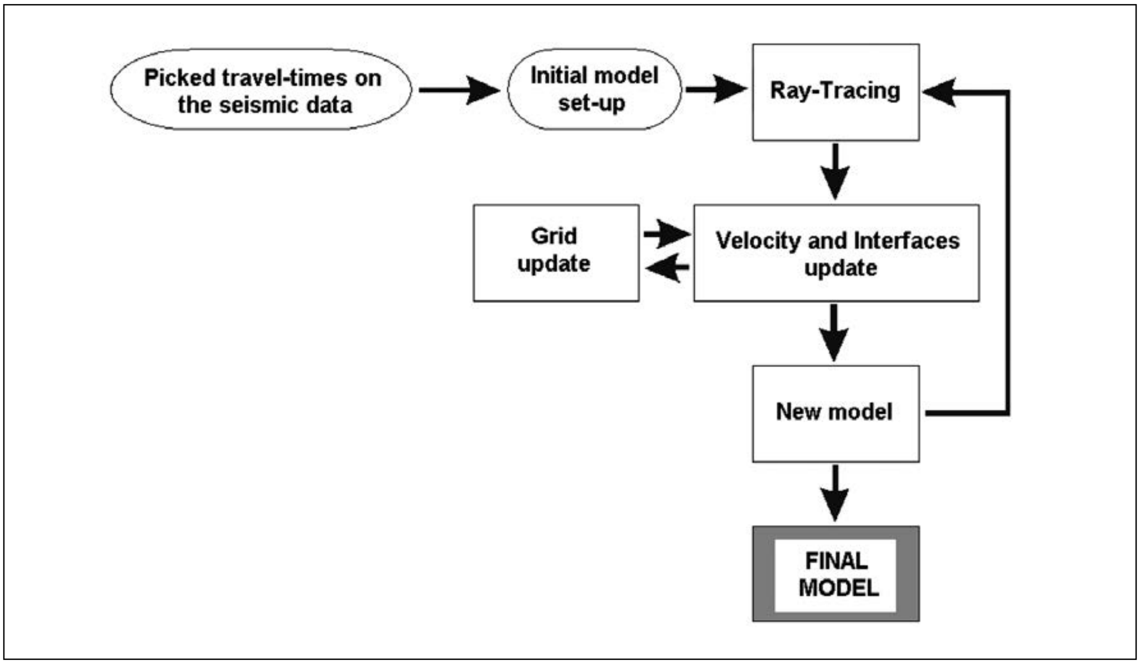

Fig. 2 - A flowchart of the travel-time tomography algorithm adopted.

3. Lake Vostok model

The synthetic model of Lake Vostok adopted for the simulations is shown in Fig. 3. The seismic properties of the model are listed in Table 1.

Table 1 – Seismic properties of the Lake Vostok model: compressional-wave (P) and shear-wave (S) velocities, density, anisotropy parameters and quality factors (Carcione and Gei, 2003). The seismic parameters of layers 1 and 2 (velocity and density) are linearly interpolated.

Layer	Medium	Depth* (m)	V_P (m/s)	V_S (m/s)	ρ (kg/m^3)	ε	δ	Q_1	Q_2
1	Firn (top)	-	1645	1089	506	0	0	30	20
1	Firn (bottom)	100	3886	1816	919	0	0	30	20
2	Blue ice 1 (top)	-	3886	1816	919	0.05	-0.1	100	80
2	Blue ice 1 (bottom)	2600	3920	1832	925	0.05	-0.1	100	80
3	Blue ice 2	2800	3820	1786	925	0.05	-0.1	100	80
4	Blue ice 3	3250	3910	1828	925	0.05	-0.1	100	80
5	Blue ice 4	3500	4120	1926	925	0.05	-0.1	100	80
6	Accreted ice (mud)	3600	3720	1735	922	0	0	60	40
7	Accreted ice (gas)	-	3709	1745	912	0	0	80	60
8	Water	-	1443	0	1017	0	0	∞	-
9	Sediments	-	2817	1530	2128	0	0	20	15
10	Bedrock	-	5200	3040	3200	0.1	0	200	180
* Base of the layer									

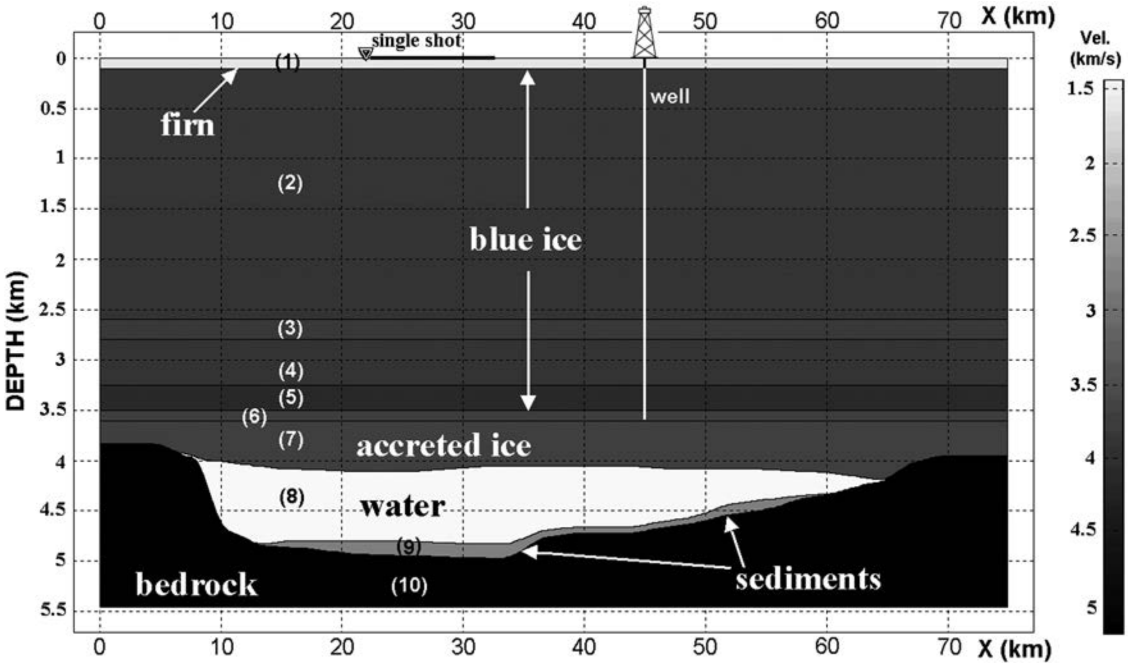

Fig. 3 - The synthetic model of Lake Vostok. The ice sheet is divided into 7 horizontal layers where the seismic parameters are horizontally constant. The depth section of the lake was derived by interpolating the RSS data acquired on Lake Vostok (section 1-1' in Fig. 1b) by the PMGRE/RAE (Kapitsa *et al*., 1996; Masolov *et al*., 1999).

We divided the ice sheet into 7 horizontal layers where the seismic parameters are horizontally constant, and the velocity and density values of layers 1 and 2 are linearly interpolated. The P-wave velocity profile of the first 6 layers were derived from a VSP at the Vostok station borehole. The depth section of the lake was derived by interpolating the RSS data acquired on Lake Vostok (section 1-1' in Fig. 1b) by the PMGRE/RAE (Kapitsa *et al*., 1996; Masolov *et al*., 1999). All the other seismic properties on Table 1 were computed by Carcione and Gei (2003) using poroelastic and viscoelastic microstructural models that take into account the *in situ* conditions of the different layers versus temperature and pressure (Carcione and Gei, 2003).

4. Wave simulations

We carried out a numerical wave simulation of a single shot in the Lake Vostok seismic model, that provided useful information (frequency of the source and AVO information) for the acquisition geometry design. For this task we adopted a wave modelling commercial package (Tesseral 2-D; Tesseral Technologies Inc.) and the seismic properties on Table 1. The offset ranges from 0 to 10 km and the source is a dilatation force, whose time-history is a Ricker wavelet. It is located at a 10 m depth, at the centre of the lake area (Fig. 3), and we tested dominant frequencies in a range from 20 Hz to 50 Hz. The wavefield is computed by using a time step of 2 ms with a maximum time of 4.5 s. A snapshot of the wavefield at 2.5 s propagation time is shown in Fig. 4. This figure gives a clear picture of the nature and location of the different events associated with the lake. For the scope of this work, the events of interest are the PP reflections related to the I-W, W-S and S-B interfaces. The direct shear wave and the PS converted wave at the I-W interface are also evident. The presence of the PS converted wave could be very useful, since it may give information on S velocities.

The synthetic shot gather of the vertical particle-velocity component recorded at the surface is shown in Fig. 5: the dominant frequency is 30 Hz, and a spherical divergence correction is applied using the velocity profile shown in Table 1. The two main PP reflection events, corresponding to the I-W and W-S interfaces at approximately 2.16 s and 3.14 s zero-offset travel-time, have opposite polarity (Carcione and Gei, 2003). The PP reflection due to the S-B interface has a zero-offset travel-time of nearly 3.24 s. Weaker reflections within the ice sheet can be seen before the I-W reflection. The straight events are the refracted waves travelling in the blue ice layer (R) and a train of direct waves travelling in the firn layer (D). Unfortunately, Rayleigh waves are not modelled by the present algorithm.

An amplitude spectral analysis (Fig. 6) of the obtained synthetic shot gather shows that there is enough energy associated to the lake top (I-W interface) and lake bottom (W-S and S-B interfaces) in correspondence to 30 Hz. So, using a dominant frequency of 30 Hz, the maximum theoretical resolution at the lake bottom is: vertical resolution = $\lambda/4 \approx 23$ m; horizontal resolution = First Fresnel Zone ≈ 1 km. Since RSS investigations on Lake Vostok (Masolov *et al.*, 1999) estimated for the sediments a thickness range from tens of meters to 350 m, a dominant frequency

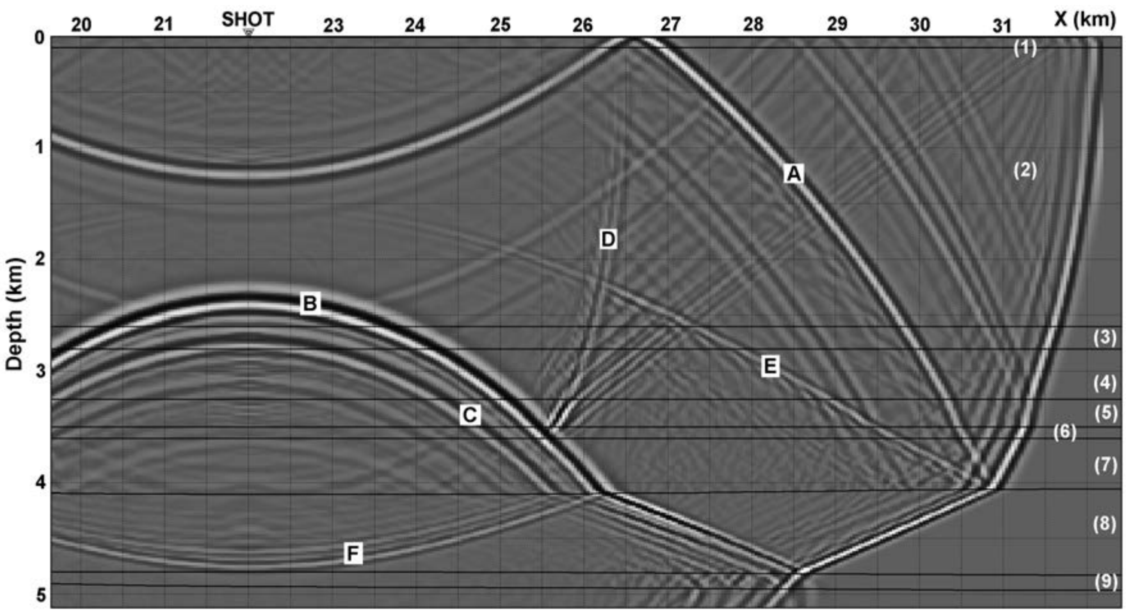

Fig. 4 – Snapshot of the vertical particle-velocity component at 2.5 s propagation time, where (A), (B) and (C) are the PP reflections at the ice-water, water-sediments and sediments-bedrock interfaces. The other events are: the direct shear wave (D), the PS converted wave at the I-W interface (E) and the reverberation inside the lake (F).

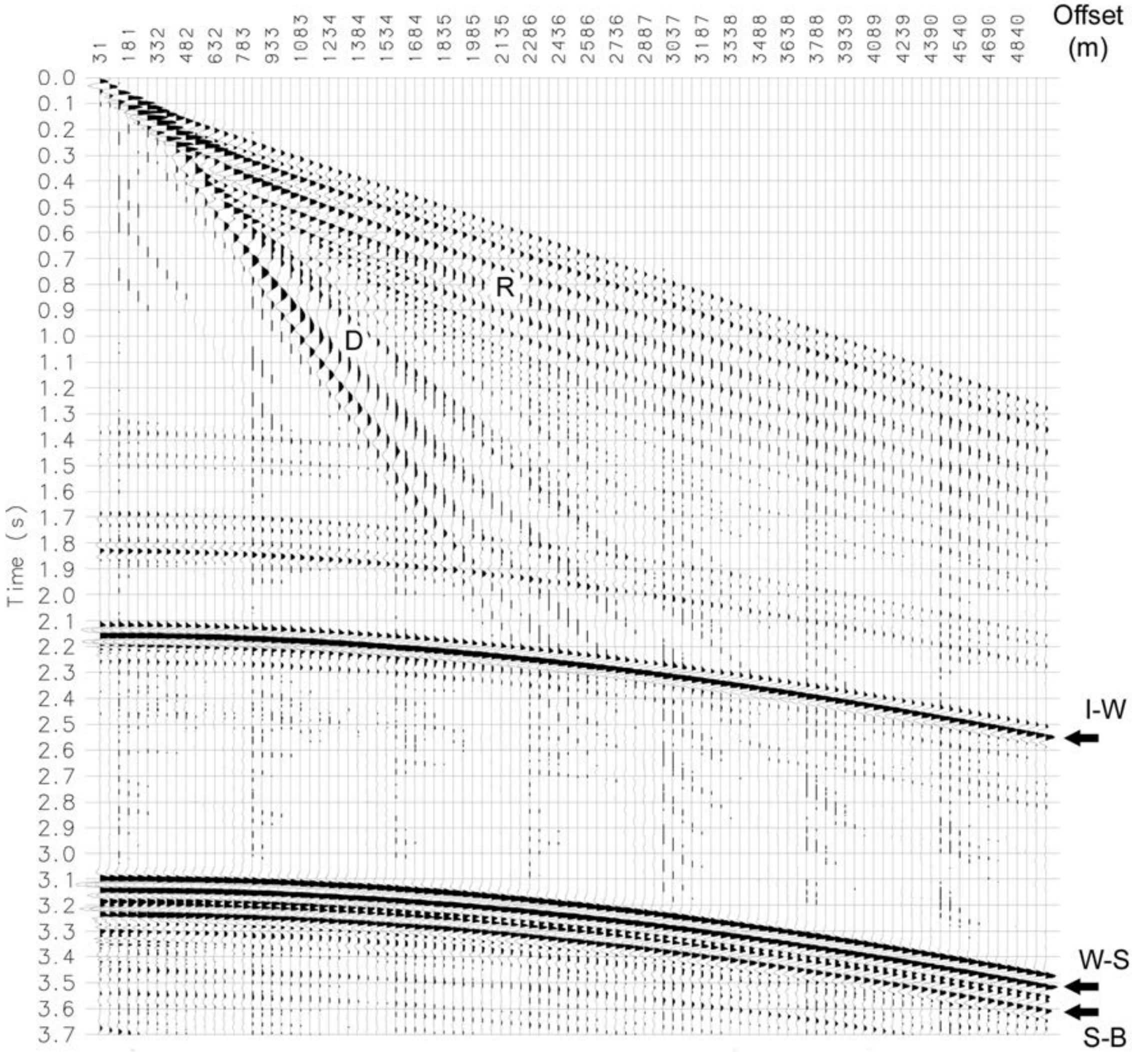

Fig. 5 – The synthetic shot gather of the vertical particle-velocity component recorded at the surface. The dominant frequency is 30 Hz, and a spherical divergence correction is applied using the velocity profile shown in Table 1. The events of interest are the PP reflections from the I-W, W-S and S-B interfaces. Weaker reflections within the ice sheet can be seen before the I-W reflection. The other events are the refracted waves travelling in the blue ice layer (R) and a train of direct waves travelling in the firn layer (D).

of 30 Hz should enable the thin layer of sediments to be characterised. A higher dominant frequency implies a greater absorption of energy in the ice layers, particularly in the firn layer, with a consequent weakening of the useful signal. On the other hand, a lower dominant frequency compromises the resolution.

Thus, we expect a real shot gather similar to the one depicted in Fig. 5, and the reflected events to be picked for the travel-time tomographic inversion are those indicated. As Carcione and Gei (2003) showed in their work, the reflections of the lake top (I-W interface) and lake bottom (W-S and S-B interfaces) show distinct characteristics, which could allow their identification in real seismic records.

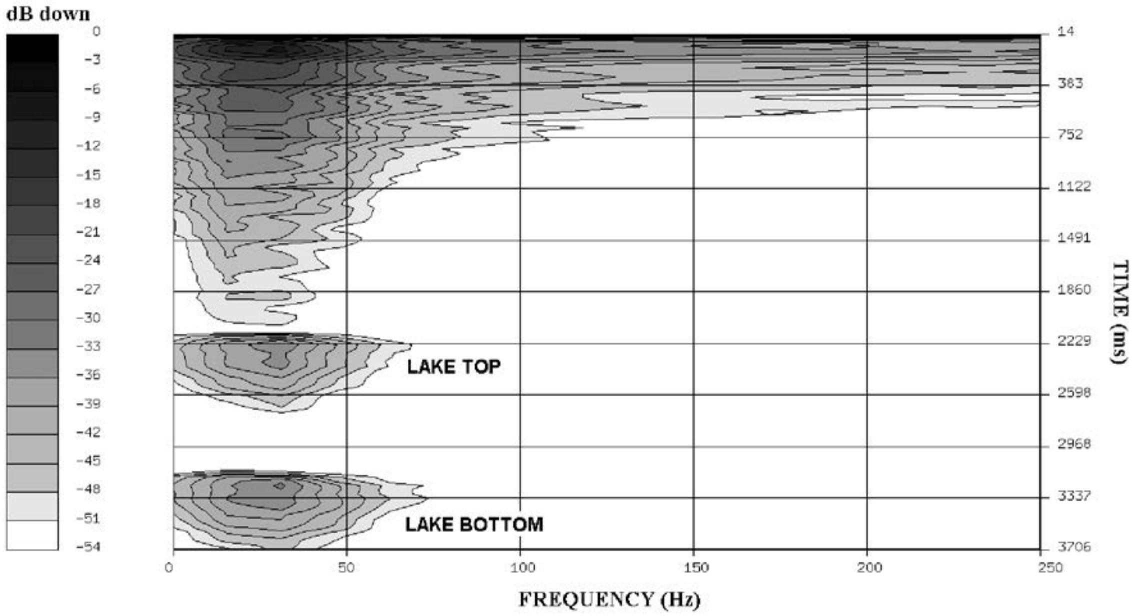

Fig. 6 – An amplitude spectra of the synthetic shot gather shown in Fig. 5. The energy associated to the lake top (I-W interface) and lake bottom (W-S and S-B interfaces) is evidenced.

5. Tomographic modelling

The modelling procedure adopted can be summarised in the following steps.

1. In the first step, we optimised the acquisition geometry and simulated the seismic survey doing a ray-tracing through the Lake Vostok model. The travel-time of the reflected arrivals related to the I-W, W-S and S-B interfaces is computed.
2. In the second step, we carried out a travel-time tomographic inversion of the reflected arrivals. Only layers 7, 8 and 9 are analysed, all the others are fixed.
3. Finally, we compared the inverse model obtained with the initial model by computing velocity and depth deviations.

We adopted a basic acquisition configuration composed of two arrays of geophones, 500 m long, the first (array A) placed near the source and the second (array B) away from the source. In this way, we have both small and high offsets, which are necessary to obtain a good velocity and depth resolution. The distances of the two arrays from the source is a compromise between the Amplitude curve and the Normal Move-Out (NMO) curve of the reflected arrivals. In Fig. 7, we plotted the Amplitude and NMO values extracted from the synthetic shot gather shown in Fig. 5, along the I-W and W-S reflected events. Since the reflectors are nearly horizontally flat in the zone of the simulation, the oscillations of the amplitude curves are related only to the seismic properties of the interfaces (Carcione and Gei, 2003). Analysing the curves, and considering that the array A can not be placed too close to the source because of the presence of the Rayleigh wave (Masolov *et al.*, 1999), the optimal S/N ratio could be obtained in the offset range from 500 m to 4.5 km. We chose a distance of 500 m for the array A, and a distance of 3 km for the array B: in this way, the mean amplitude related to the array A is maximum, and the mean amplitude related to the array B is nearly half of the maximum amplitude (for each reflection event). Moreover, as required for a faithful tomographic inversion, we have a small NMO for the array A, and a large NMO for the array B (the mean NMO ratio between B and A is 15). The two highlighted intervals A and B, in Fig. 7, indicate the position of the two arrays with respect to the source.

In Fig. 8, the acquisition procedure is described: shifting both source and arrays 1 km away after each shot and employing 6 geophones at 100 m spacing for each array, we are able to obtain a sufficient ray coverage (fold) at the bottom of the lake. A single shot ray-tracing of the reflections related to the S-B interface is illustrated in Fig. 9: since the velocity of the ice is greater than the velocity of water, the angle of transmission at the I-W interface is lower than the angle of incidence. Moreover, according to Snell's law, there is no critical angle at the I-W interface and the critical angle at the W-S interface is nearly 31°. Since the maximum horizontal resolution at the lake bottom is about 1 km (see previous section), we calculated the fold at the W-S and S-B interfaces using 1 km width pixels. The resulting fold ranges from 6 rays/km to 8 rays/km. It is rather low but, as shown in the next section, high enough to faithfully recover the geometry of the lake.

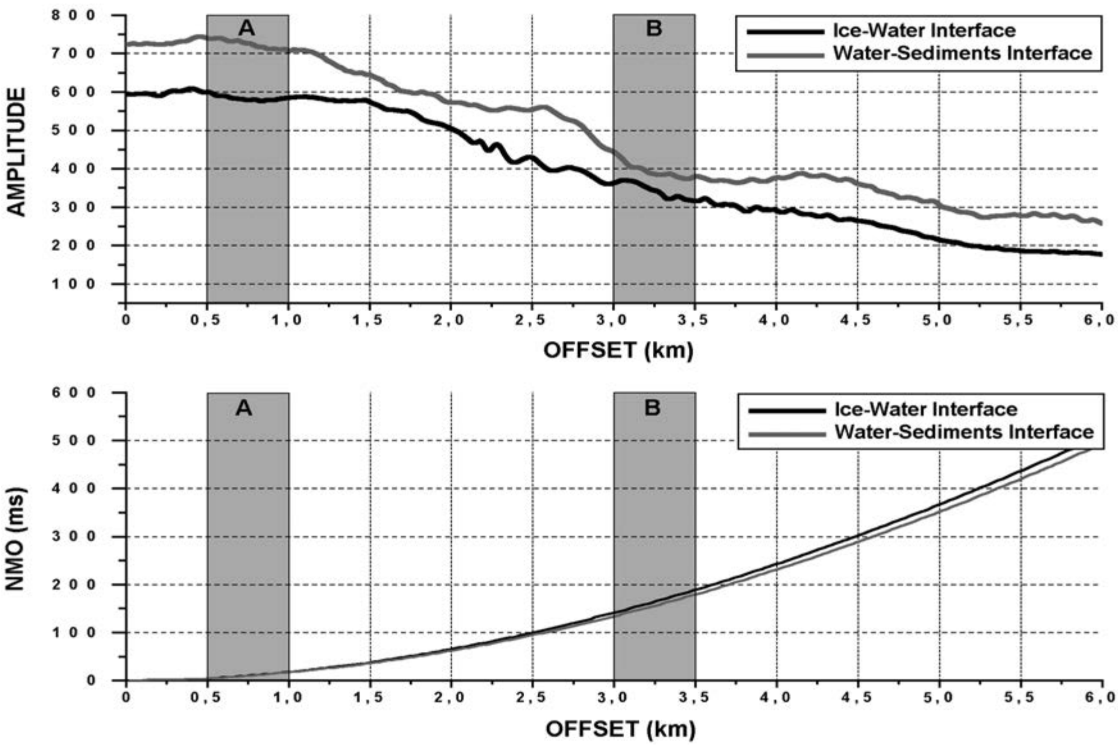

Fig. 7 – Amplitude and NMO curves extracted from the synthetic shot gather of Fig. 5, along the I-W and W-S reflected arrivals. The highlighted intervals A and B show the position of the two arrays with respect to the source. The mean amplitude on B is about half of the mean amplitude on A (for each reflection event). The mean amplitude ratio between the I-W and W-S reflections is 0.8 on A and 0.82 on B. The mean NMO difference is 0.47 ms on A and 8.48 ms on B. The mean NMO ratio between B and A is about 15.

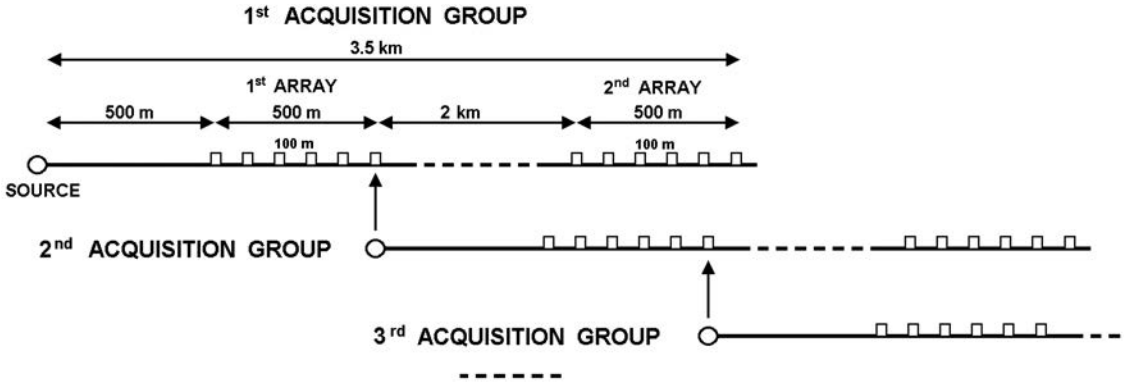

Fig. 8 – Displacement of the seismic acquisition groups along the profile. The number of shots is 75, at 1 km spacing, and both source and arrays are shifted away after each shot. With a receiver interval of 100 m the fold at the bottom of the lake ranges from 6 rays/km to 8 rays/km.

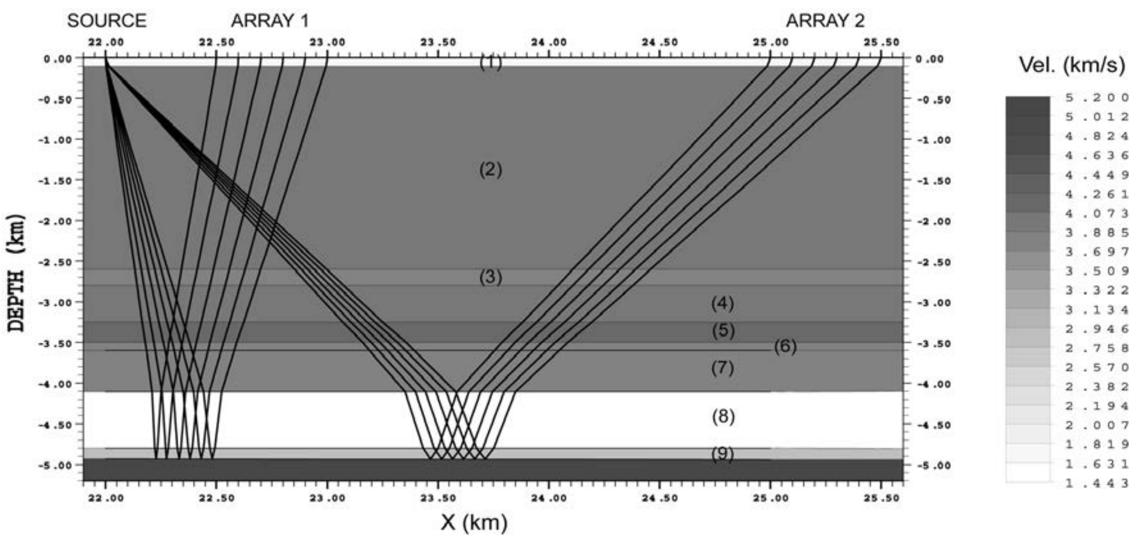

Fig. 9 – A single shot ray-tracing of the reflections related to the S-B interface. According to Snell's law, the velocity inversion at the lake reduces the transmission angle at the I-W interface and there is no critical angle. The critical angle at the W-S interface is nearly 31°.

6. Results of the tomographic inversion

The inverted model, result of the tomographic inversion, is shown in Fig. 10a. We quantified the imperfections by computing the velocity and depth deviations between the original model (Fig. 3) and the inverted model. The velocity deviations are plotted directly on the pixels of the inverted model (Fig. 10a), while the depth deviations are shown in Fig. 10b.

The larger imperfections are in correspondence with the bottom of the lake: we obtained low velocity deviations in the accreted ice layer and in the water layer, and high velocity deviations in the sediments layer. This is principally due to the fact that the sediments layer is very much thinner than the other two inverted layers. The maximum velocity deviation is 130 m/s, corresponding to the central slope of the sediments layer, while the maximum (but isolated) depth deviation is 160 m, corresponding to the lateral slope of the lake. The total velocity deviation, computed as mean of the absolute deviation values of the three layers, is 47.5 m/s. Moreover, the total depth deviation is 16.3 m, i.e., about 0.4 % of the mean depth related to the I-W, W-S and

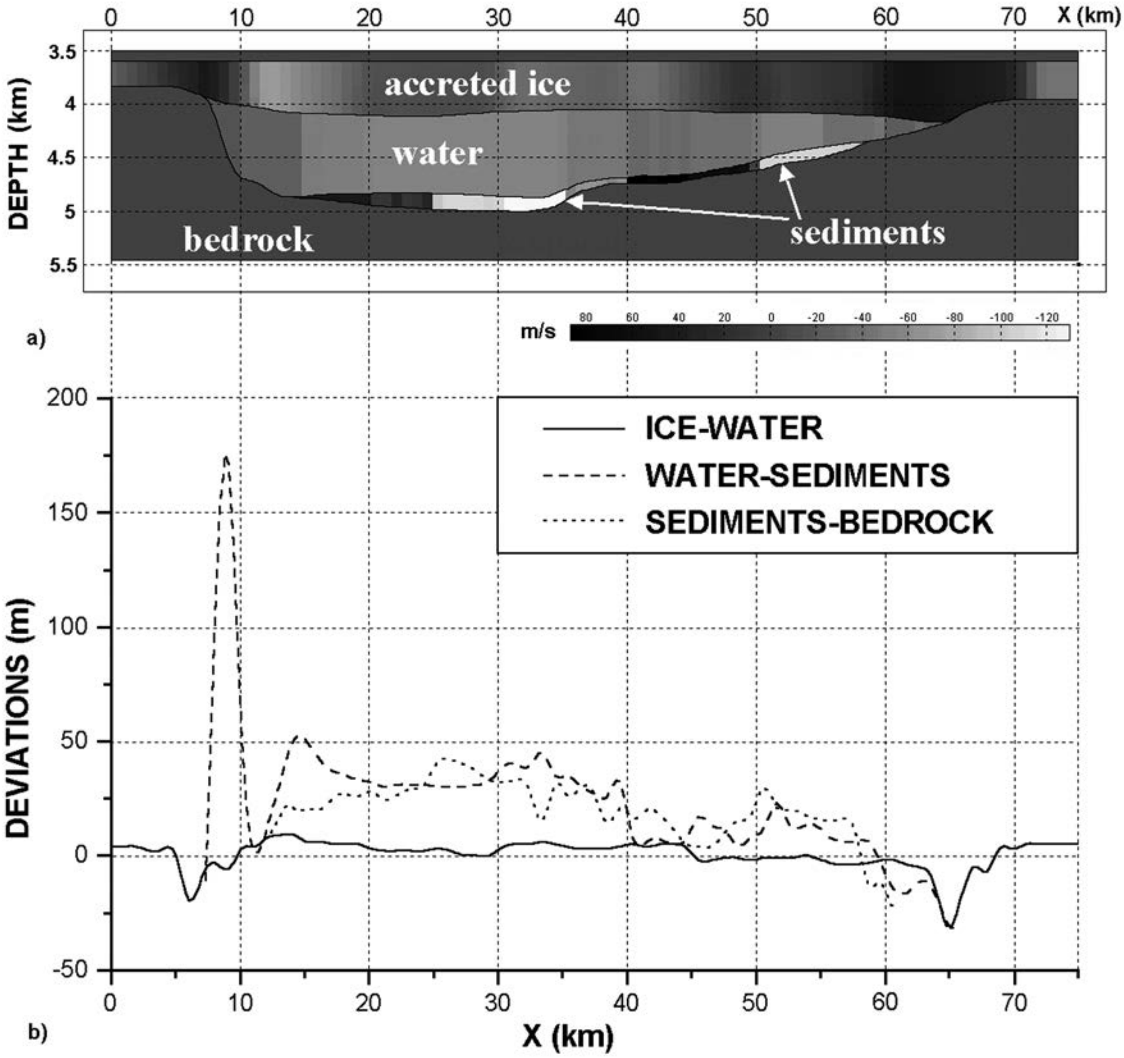

Fig. 10 - a) Velocity deviations of the three inverted layers. The maximum deviation is 130 m/s, corresponding to the central slope of the sediments layer. The total deviation, computed by means of the absolute deviation values related to the three layers, is 47.5 m/s. b) Depth deviations of the three inverted interfaces. The maximum deviation is 160 m, corresponding to the lateral slope of the lake. The total deviation is 16.3 m, i.e., about 0.4% of the mean depth related to the three interfaces.

S-B interfaces. The mean velocity and thickness deviations of each layer are shown in Table 2 while the mean depth deviation of each interface is shown in Table 3.

Table 2 - Velocity and thickness deviations of each layer, computed as mean of the absolute deviation values. The Layer Velocity (LV) values and Mean Layer Thickness (MLT) values are those of the original model shown in Fig. 3.

	Accreted ice layer	**Water layer**	**Sediments layer**
Mean Velocity Deviation (MVD)	32 m/s	42 m/s	87 m/s
$\frac{MVD*100}{LV}$	0.8 %	2.9 %	3.1 %
Mean Thickness Deviation (MTD)	4.5 m	22.8 m	9.2 m
$\frac{MTD*100}{MLT}$	1 %	4.8 %	11 %

Table 3 - Depth deviations of each interface, computed as mean of the absolute deviation values. The Mean Interface Depth (MID) values are those of the original model shown in Fig. 3.

	Ice-Water interface	**Water-Sediments interface**	**Sediments-Bedrock Interface**
Mean Depth Deviation (MDD)	4.5 m	26.1 m	26.8 m
$\frac{MTD*100}{MID}$	0.1 %	0.6 %	0.5 %

Finally, we estimated how much the result would be improved by doubling the number of shots. We simulated an acquisition employing 150 shots, at 500 m spacing, and performed the tomographic inversion. The total depth deviation decreases by 25%, while the maximum improvement occurs in correspondence to the W-S interface (Fig. 11), for which the mean depth deviation decreases by 27%.

7. Conclusions

Numerical modelling of wave propagation and travel-time reflection tomography were applied to design a multichannel seismic reflection survey aimed at recovering the Antarctic subglacial lake geometry. The designed seismic survey fulfils the main goal of this work which was to achieve a good compromise between the costs of the survey execution and the information that could be extracted from the acquired seismic data. The tomographic inversion showed that if the survey is carried out by adopting the acquisition geometry illustrated in Fig. 8, and the seismic data interpreted correctly (Carcione and Gei, 2003), the geometry of Lake Vostok can be recovered with an acceptable accuracy.

The total depth deviation (computed as mean of the absolute deviation values of the I-W, W-S and S-B interfaces) is 16.3 m, i.e., about 0.4% of the mean depth related to the three interfaces. Moreover, the mean thickness deviation of the sediments layer is 9.2 m, i.e., 11% of the mean

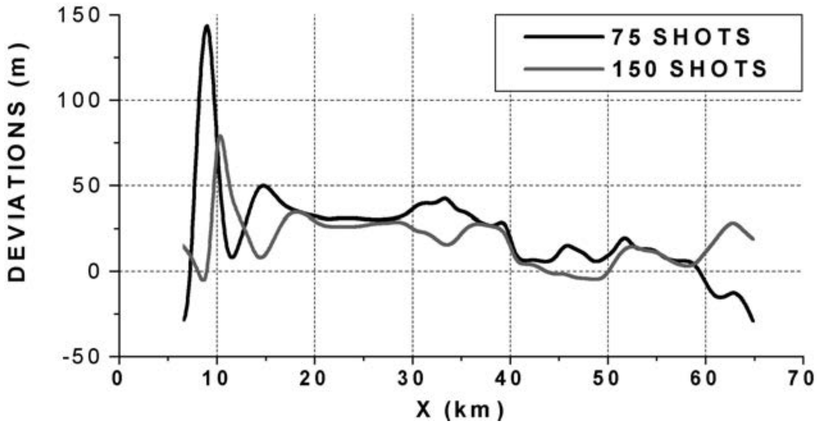

Fig. 11 - Depth deviations of the W-S Interface. Doubling the number of shots the mean depth deviation of this interface decreases by 27%.

thickness of the layer. The mean velocity and thickness deviations of the other layers are shown in Table 2 while the mean depth deviation of each interface is shown in Table 3. By doubling the number of shots, the total depth deviation decreases by 25%. This improvement is significant, but we think that it is not sufficient to justify a doubling of the effort in order to carry out the survey.

Acknowledgements. This work was presented at the 22nd GNGTS Conference. The author would like to thank all the staff of the REDAS group at OGS and Tesseral Technologies Inc. for their contribution.

REFERENCES

Carcione J.M. and Gei D.; 2003: *Seismic modelling study of a subglacial lake.* Geophysical Prospecting, **51**, 501-515.

Kapitsa A.P., Ridley J.K., Robin G. de Q., Siegert M.J. and Zotikov I.A.; 1996: *A large deep freshwater lake beneath the ice of central East Antarctica*. Nature, **381**, 684-686.

Masolov V.N., Kudryavtzev G.A., Sheremetiev A.N., Popkov A.M., Popov S.V., Lukin V.V., Grikurov G.E. and Leitchenkov G.L.; 1999: *Earth science studies in the Lake Vostok region: existing data and proposals for future research*. In: SCAR International Workshop Report on Subglacial Lake Exploration, Cambridge, England, **2**, 1-18.

Siegert M.J.; 2000: *Antarctic subglacial lakes*. Earth Science Reviews, **50**, 29-50.

Siegert M.J., Dowdeswell J.A., Gorman M.R. and McIntyre N.F.; 1996: *An inventory of Antarctic subglacial lakes*. Antarctic Science, **8**, 281-286.

Vesnaver A., Böhm G., Madrussani G., Petersen S. and Rossi G.; 1999: *Tomographic imaging by reflected and refracted arrivals at the North Sea*. Geophysics, **64**, 1852-1862.

Corresponding author: Stefano Picotti
Istituto Nazionale di Oceanografia e di Geofisica Sperimentale - OGS,
Dipartimento di Geofisica della Litosfera;
Borgo Grotta Gigante 42/c, 34010 Sgonico (Trieste), Italy
phone: +39 0402140295; fax: +39 040327307; e-mail: spicotti@ogs.trieste.it